

**Orest BILYY, Jorge GONZÁLEZ-SÁNCHEZ, Luis DZIB-PÉREZ,  
Juliana ROSADO CARRASCO, Gabriel CANTO**

## **TO ASSESSMENT OF DEFECTS DEVELOPMENT OF WELDED JOINTS STAINLESS STEEL DUPLEX 2205**

*Centre for Corrosion Research, Autonomous University of Campeche,  
Av. Agustín Melgar s/n, Col. Buenavista, 24039, Campeche, Mexico  
E-mail: bilorestl@gmail.com*

Local corrosion-mechanical and corrosion damage of various objects substantially affects their service life, as well as the residual lifetime under operating conditions. In this paper, we propose analytical correlations for corrosion current density of different parts of the welded joint, namely the base material, the heat-affected zone and directly the material of the weld. These ratios are used to construct dependences for development of corrosion pits and defects of welded joints stainless steel duplex 2205. This model was implemented on the basis of experimental studies that were conducted on samples made of real objects. The work analyses the distribution of the corrosion current density in each of the components of the welded joint. The conclusions are formulated on the basis of consideration of experimental researches and on the basis of the proposed numerical-analytical model. With the help of the proposed model, one can find implicit dependence of the behaviour of the objects in the system. The obtained results can be used further in the study of kinetics of growth of local corrosion damage in the considered objects.

**KEY WORDS:** *stainless steel duplex, welded joints, corrosion current density, mechanochemical and corrosive damages, numeric-analytical model.*

### **INTRODUCTION**

Duplex stainless steel (DSS) 2205 is an alloy containing 22% of Cr and 5% of Ni. Its microstructure is a matrix of  $\delta$ -ferrite BCC with  $\gamma$ -austenite FCC grains islands in a 50/50 ratio. DSS is used in industry due its high mechanical strength and corrosion resistance, better than ferritic or austenitic stainless steels [1–3]. However, most structures or components contain welding joints and this changes the  $\delta/\gamma$  microstructural balance. Also detrimental phases such as  $\sigma$  or  $\chi$ , besides carbides or nitrides can precipitate. The formation of these phases weakens the passive film due to Cr depletion at the adjacent zones surrounding, this increases the localized corrosion susceptibility and it is said that the steel has been sensitized [4].

As mentioned above, the formation of intermetallic phases in the temperature range of 750-950 ° C leads to a significant loss of impact strength, compressive plasticity due to fracture and fracture toughness, which reduces friction due to their poor deformability, as well as their morphology [5, 6].

Although post-welding thermal processing is widely used in the industry to dissolve such disastrous phases and residual stresses, it leads to expensive, labor-intensive and impractical for large structures or components [7–9].

The use of electromagnetic fields at AISI 304 stainless steel gas metal arc welding (GMAW) has been reported with very good results in improving corrosion resistance [10].

There are three main zones at welding joints: base metal (BM), fusion zone (FZ) which is formed of filler metal and heat affected zone (HAZ) that is adjacent to FZ and is where most of the microstructural changes take place. Post welding heat treatments are common practice to minimize sensitization issues, this works for small components, however, for large structures it's very expensive and it's not feasible to do. This research work assesses the effect of the application of a 3 mT external magnetic field (EMF) during GMAW of DSS 2205 in terms of microstructural evolution associated to welding thermal cycles and localized corrosion resistance.

### **METHODOLOGY**

**Welding procedure.** GMAW was carried out using AISI 2205 DSS plates with single ‘V’ groove configuration and dimensions were 6×70×150 mm, as shown schematically in Fig. 1.

As shielding gas a 98% Ar + 2% O<sub>2</sub> mix flowing at 17 L/min and a wire of filler metal ER-2209 with a 1.2 mm diameter fed at 160 mm/s were used. Operating variables of the process were set in order to obtain a heat input of 1.4 kJ/mm considering an efficiency of 75% and a welding speed of the torch at 3.6 mm/s. To apply the EMF of 3 mT during welding was used an experimental set up, consisting in a 3 wire coil and an external power supply as shown in Fig. 2 [4].

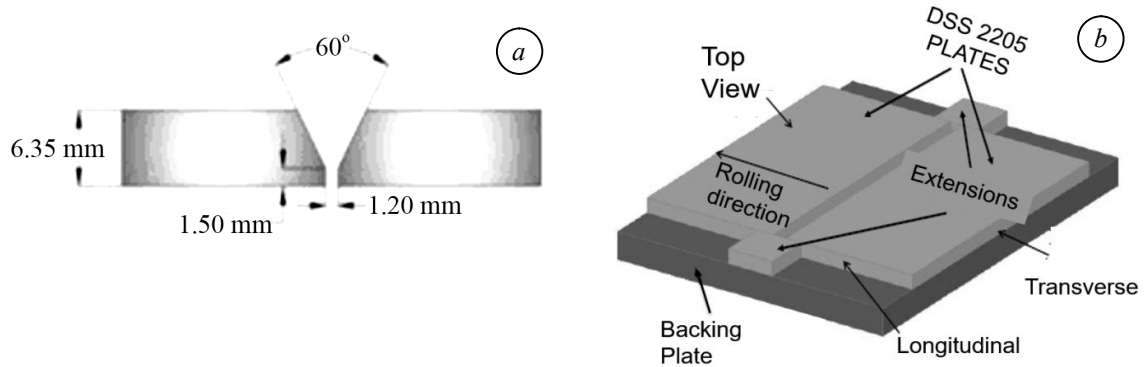


Fig. 1. Schematic diagram of welding joint configuration Single V-Groove (a) and isometric view (b) [4].

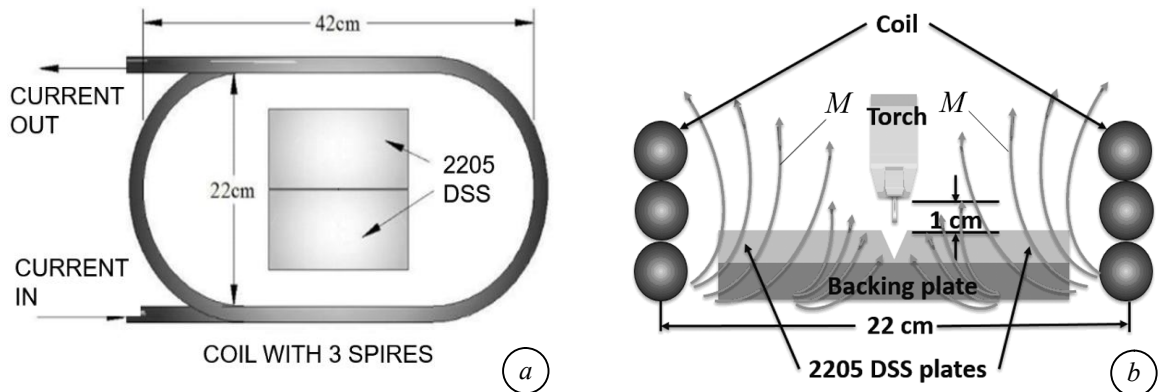


Fig. 2. Application of electromagnetic field during GMAW: geometric set up (a) and transversal section (b). *M* – represent magnetic field lines.

**Localized corrosion assessment.** Electrochemical tests were carried out in order to assess localized corrosion resistance in terms of degree of sensitization (DOS), electrochemical behaviour in natural sea water and critical pitting temperature (CPT) evaluation in natural sea water too. Specimens were fabricated by transversal cut-off of the welding joints containing part of BM, HAZ and FZ. Also BM specimens as-received condition were obtained. The cut-of were embedded into epoxy resin and an electrical wire was attached.

A three-electrode conventional electrochemical cell was arranged, using a saturated calomel electrode as reference electrode, a graphite bar was the auxiliary electrode and specimens were the working electrodes. Specimens were grounded with progressive SiC paper up to 1200 grit. To assess electrochemical behaviour in natural sea water, the specimens surface was also polished with 1  $\mu$ m diamond paste. Then all the specimens were rinsed with deionized water and degreased with acetone. The three electrodes were connected to a Solartron SI 1287 potentiostat/galvanostat.

DOS were determined by using double loop electrochemical potentiokinetic reactivation (DL-EPR) technique which consists in the activation potentiodynamic polarization applying an anodic overpotential  $\eta_a = 600$  mV from the open circuit potential (OCP) with a 1 mV/s scanning rate and then a reverse polarization is performed that could induce a reactivation. To calculate DOS the value  $I_r/I_a$  ratio is obtained where  $I_r$  is the maximum current density peak resulting from the reactivation polarization and  $I_a$  is the maximum current density peak of the activation polarization [11]. Electrolyte 2 M H<sub>2</sub>SO<sub>4</sub> + 1 M HCl solution at 30°C was used, as Gong et. al. suggest [12] for AISI

2205 DSS. Electrochemical behavior in natural sea water was assessed at a temperature of 25°C by a Potentiodynamic Polarization going from a cathodic over potential  $\eta_a = 900$  mV vs OCP with a scanning rate of 0.167 mV/s. According to the ASTM-G150-99 norm, a potentiostatic polarization was conducted to determine CPT in natural sea water setting an overpotential of 750 mV vs ESC with a gradual temperature rising of 1°C/min going from 10°C until a peak of current density suddenly reaches a value  $i = 100 \mu\text{A}/\text{cm}^2$  [13]. This was achieved by using a thermostatic heating plate and a magnetic agitator. The electrochemical cell was placed in a water bath in order to maintain a homogeneous temperature. At the end of every test, an optical microscopy analysis was carried out.

Table 1. Mean values of microhardness Vickers HV 0.2 for the phases of duplex stainless steel 2205

Conditions	HV 0.2
$\delta$	317.18
$\gamma$	306.38
MB	313.54

Vickers microhardness tests (HV 0.2) were performed to measure the differences between the  $\delta$  and  $\gamma$  phases of the base metal, as well as for the different areas of the welded joints with and without magnetic field. As can be seen in Table 1, the values for  $\gamma$  phase are between 283 and 320, while for  $\delta$  phase the results show values between 308 and 338. These results are very close to that reported in other investigations and agree that, although the microhardness values are similar in both phases, in the case of  $\delta$  phase it is slightly greater than in the  $\gamma$  phase [4]. The mean value taken into consideration both phases

is 313. The measurements were made on the base metal as arrived condition.

The results of the measurements in the areas of the welded joint indicate that for the three applied magnetic field strengths the weld metal has a higher microhardness than for other zones, the thermally affected area having the lowest hardness. This may be due to the fact that the weld metal contains a higher percentage of Ni than the base metal, since, as established in [12], this alloy element increases the hardness.

As can be seen in Fig. 3, the microhardness values are very similar for 0 and 3 mT, while welding with 12 mT has higher values. García [4] reported similar results for welding with a magnetic field of 12 mT and he attributed this increase to the decrease in ferritic grain size due to electromagnetic stirring. Although the 3 mT weld would be expected to have a higher microhardness than the 0 mT weld, the similarity of the results can be attributed to the fact that the amount of  $\delta$  phase is greater than in the 0 mT weld.

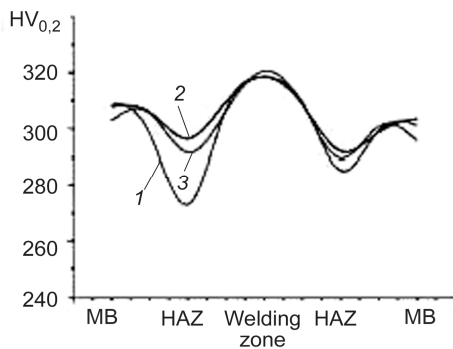


Fig. 3. Microhardness profiles for three welding conditions. The sweep was carried out in the cross section of the welded joints: 1 – 0 mT; 2 – 3 mT; 3 – 12 mT.

On the other hand, the reduction of microhardness in the HAZ can be attributed to the increase in the size of ferritic grains, as reported by other researchers [4, 12], the temperature reached in this area allows the coalescence of them. However, the microhardness in the HAZ of the 3 mT weld is higher than that of the welded joints of 0 mT, which coincides with that reported by García [4].

The microstructural characteristics evaluated in this section are related to the electrochemical behavior and to the fatigue cracking resistance, as it will be seen below. In the following section the results of the electrochemical tests carried out in welded joints will be found, evaluating the three zones in an integral way. In the work carried out by García [4] electrochemical tests were performed isolating each of the welding parts to evaluate the electrochemical and mechanical properties separately. This will be very useful as a first approximation to have a better understanding of the aspects evaluated below.

Also in this work the welded joints as a three-electrode electrochemical system, an analytic procedure for the evaluation of corrosion current density distribution at the welded zone is proposed. On this basis the experimental–numerical method for prediction of profile and maximum depth of local corrosion defects in the components of welded joints has been developed. The data on general characterization and maximal depth of localized damaging on surface of parts of welded joints were received and analyzed with dependence of term exploitation and composition of operating environment. In particular, the possibility of changing the polarity of local galvanic couples in the vicinity of the welding zone depending on the period of operation has been shown and that cannot it can not be predicted within the framework of the existed approaches.

The indicated model scheme of combined welded joints is used as basic for the development of the numerical–analytic procedure of determination of the density of corrosion current on the surface of the welded zone. This scheme is realized according to the method of equalized polarization [14]. To do this, it is necessary first to establish some specific features of the exact solution of the posed problem.

In the rigorous statement of the problem, the current density is analytically determined via the electric potentials of the medium  $\psi_n(r, Z)$  satisfying the Laplace equation [14]:

$$\left( \frac{\partial^2}{\partial r^2} + \frac{1}{r} \frac{\partial}{\partial r} + \frac{\partial^2}{\partial Z^2} \right) \psi_n(r, Z) = 0 \quad n=1,2,3. \quad (1)$$

Thus, if we take into account the fact that the conductivity of the metals is  $10^6 \dots 10^7$  times higher than the conductivity of the medium, then it is possible to assume that the electric potential of the metal surface

$$\psi_m \approx \text{const} = 0 \quad (2)$$

Then the process of anodic dissolution of alloys is characterized by the absence of any significant selective dissolution of individual components [15]. Thus, to predict the development of corrosion–induced defects of welded joints, we get the following dependence of the corrosion rate (m/s) on the parameters of the alloy:

$$v(Z) = \frac{1}{F \cdot D} \cdot \frac{i(Z, E, \kappa)}{\sum_{p=1}^P \frac{d_p \cdot n_p}{A_p}} \quad (3)$$

where  $p$  is the number of a component;  $d_p$  is its relative mass content;  $A_p$  is the mass of an atom of the component in atomic units;  $n_p$  is the valency of the metal;  $P$  is the number of components;  $D$  is the density of the alloy;  $F$  is the Faraday constant.

Proposed model and received data can be served as basis for prediction of the given welded joint behavior during long-term exploitation with the aim to prevent the catastrophic situations.

## RESULTS AND DISCUSSION

**Degree of sensitization.** The value of  $I_r/I_a = 0.001$  ratio was used as boundary between a sensitized material ( $I_r/I_a > 0.001$ ) and non-sensitized one ( $I_r/I_a < 0.001$ ) [11] comparing with DOS of BM as-received condition, conventional welding and joints welded under Electromagnetic Interaction of Low Intensity (EMILI) 3 mT.

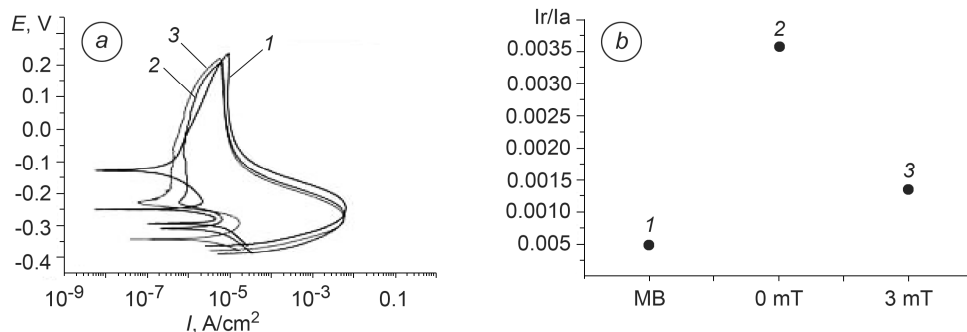


Fig. 4. DL-EPR diagram for every welding condition (a) and  $I_r/I_a$  ratio (b): 1 – AR; 2 – 3 mT; 3 – 0 mT.

DOS measurements for each condition show that the largest DOS value is for conventional welding and the smallest one is for the BM in as-received condition. For the 3 mT welding joint, it can be observed in Fig. 4 that the DOS value is smaller than conventional welding but it is still larger than BM as-received condition. These results are concerning with those reported by García et al. [4, 16]. DOS values are shown in Table 1.

**Electrochemical behaviour in natural sea water.** As a result of potentiodynamic polarization for each specimen, a very similar kinetic behavior can be observed, all specimens remain passive in an anodic potential window of 400 mV approximately. Later, at values after 870 mV, transpassive dissolution takes place but there's no stable pitting as shown in Fig. 5.

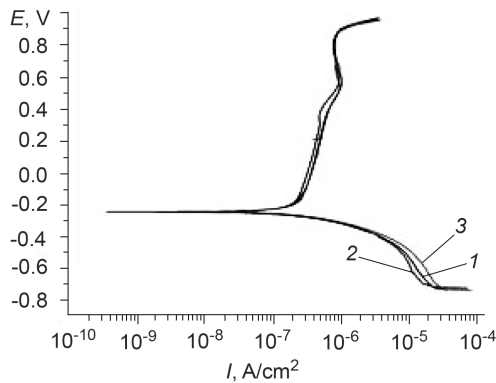


Fig. 5. Electrochemical behaviour welding joints:  
1 – MB; 2 – 0 mT; 3 – 3 mT.

Table 2.  $I_r/I_a$  ratio values for every condition of welding

Welding condition	$I_r/I_a$ (DOS)
MB	0.0005
0 mT	0.0035
3 mT	0.0013

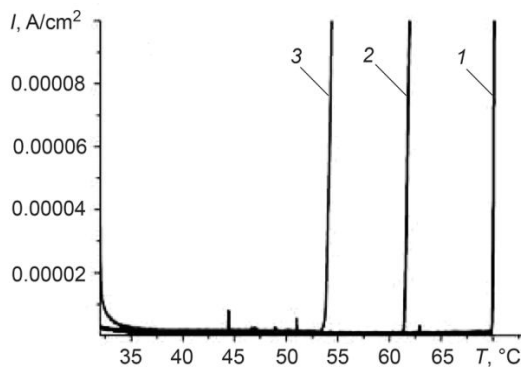


Fig. 6. Resulting chronoamperometry from potentiostatic polarization:  
1 – MB; 2 – 3 mT; 3 – 0 mT.

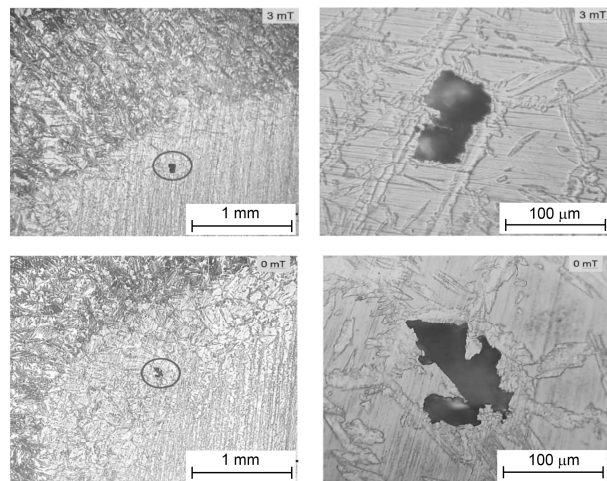


Fig. 7. Pittings at HAZ of weldings.

**Critical pitting temperature.** Values of temperature were calculated based on chronoamperometry obtained from the tests. Results show that the higher CPT (69.5°C) is for the BM in as-received condition, followed for the specimen welded under EMILI of 3 mT (61°C) and the lowest CPT (54°C) is for the specimen welded without EMILI. These results are shown in Fig. 6. The optical microscopes after the tests are shown in Fig. 7.

## CONCLUSIONS

It can be concluded from this research work that external electromagnetic interaction of 3 mT applied during GMAW process of AISI 2205 Duplex stainless steel leads to an increase of localized corrosion resistance in terms of IGC reducing the DOS. Likewise, it also improves the pitting corrosion resistance in chloride ion containing environments. On the other hand, although EMILI of 3

mT is applied, HAZ is more susceptible to localized corrosion meanwhile the phase that undergoes a preferential dissolution is  $\delta$ -ferrite. In this work the analytical–numerical model of calculation of defects on the different surface of welded joint is proposed.

#### REFERENCES

1. Short crack nucleation and growth in lean duplex stainless steels fatigued at room temperature / R. Strubbia, S. Hereñú, M. C. Marinelli, and I. Alvarez–Armas // *International Journal of Fatigue*. – 2012. – V. 41. – P. 90–94.
2. *Stainless Steels*, Scientific editors: Lacombe P., Baroux B. and Beranger G. / Les editions de physique: Les Ulis Cédex, France – 1993.
3. Nilsson J.-O. Super Duplex Stainless Steel // *Materials Science and Technology*. – 1992. – Vol. 8, № 8. – 1992. – P. 685–700.
4. Electrochemical Characterization of AISI 2205 Duplex Stainless Steel Welded Joints with Electromagnetic Interaction / M.A. García Rentería, R. García Hernández, E. Bedolla Becerril, J.A. González Sánchez // *International Congress of Science and Technology of Metallurgy and Materials*. – SAM –CONAMET. – 2013.
5. Pohl M., Storz O., Glogowski T. Effect of intermetallic precipitation on the properties of duplex stainless steel // *Materials Characterization*. – 2007. – Vol. 58. – P. 65–71.
6. Solomon H. D. Age hardening in a duplex stainless steel // *J. of Heat Treating*. – 1983. – P. 3–15.
7. Voronenko B. I. Austenitic-ferritic stainless steels: A state of art review // *Metal. Sci. and Heat Treatment*. – 1997. – Vol. 39. – P. 428–437.
8. Effect of post-weld heat treatment on microstructure evolution and pitting corrosion behaviour of UNS S31803 duplex stainless steel welds / Z. Zhang, Z. Wang, Y. Jiang, H. Tan, D. Han, Y. Guo, J. Li. // *Corrosion Sci.* – 2012. – Vol. 62. – P. 42–50.
9. Effect of a brief post-weld heat treatment on the microstructure evolution and pitting corrosion of laser beam welded UNS S31803 duplex stainless steel / Y. Yang, Z. Wang, H. Tan, J. Hong, Y. Jiang, L. Jiang, J. Li // *Corrosion Sci.* – 2012. – Vol. 65. – P. 472–480.
10. Effect of magnetic field applied during gas metal arc welding on the resistance to localized corrosion of the heat affected zone in AISI 304 stainless steel / F.F. Curiel, R. García, V.H. López, J. González-Sánchez // *Corrosion Sci.* – 2011. – Vol. 53. – P. 2393–2399.
11. Martínez E. A. Corrosión por Picaduras y Sensibilización de las técnicas electroquímicas aplicadas al estudio de la corrosión en la industria nuclear. – 2002.
12. Evaluation of intergranular corrosion susceptibility of UNS S31803 duplex stainless steel with an optimized double loop electrochemical potentiokinetic reactivation method / Gong Jia, Y.M. Jianga, B. Denga, J. L. Xua, J. P. Hub, Lia Jin // *Electrochimica Acta*. – 2010. – Vol. 55, № 18. – P. 5077–5083.
13. ASTM “Standard Test Method for Electrochemical Critical Pitting Temperature Testing of Stainless Steels” ASTM G150-99. – 1999.
14. Iossel Yu. Ya. and Klenov G. É. *Mathematical Methods for the Assessment of Electrochemical Corrosion and Protection of Metals. A Handbook* [in Russian]. – Moscow: Metallurgiya, 1984.
15. Investigation of the development of localized corrosion-induced defects of welded pipes of elements of the water-steam channels of thermal electric power plants / I.M. Dmytrakh, O.L. Bilyi, B.I. Kolodii, R.L. Leshchak // *Materials Science*. – 2006. – Vol. 42, № 4. – 2006. – P. 440–450.
16. Improvement of localized corrosion resistance of AISI 2205 Duplex Stainless Steel joints made by gas metal arc welding under electromagnetic interaction of low intensity / M.A. García-Rentería, V.H. López-Morelos, R. García-Hernández, L. Dzib-Pérez, E. M. García-Ochoa, J. González-Sánchez // *Applied Surface Science*. – Elsevier. – 2014. – Vol. 321. – P. 252–260.